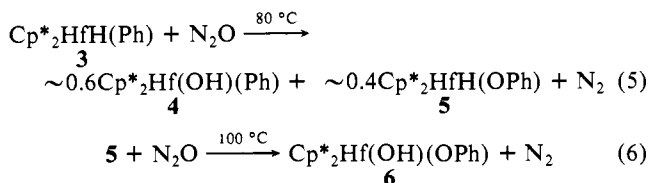


temperatures (100 °C) or longer reaction times (12 h) **5** reacts with N<sub>2</sub>O to give N<sub>2</sub> and the mixed hydroxyphenoxy complex Cp\*<sub>2</sub>Hf(OH)(OPh) (**6**),<sup>11</sup> shown in eq 6, but **4** does not react with



N<sub>2</sub>O below its decomposition temperature (140 °C).<sup>12</sup> The oxidation of the phenyl and hydride ligands of **3** at comparable rates argues against an insertion mechanism for N<sub>2</sub>O activation analogous to that seen for RN<sub>3</sub> and R<sub>2</sub>CN<sub>2</sub> (eq 3 and 4). While the intermediacy of [Cp\*<sub>2</sub>Hf(ONNH)(Ph)] in the formation of **4** is plausible, [Cp\*<sub>2</sub>HfH(ONNPh)] is not a reasonable precursor to **5** because of the high activation barrier expected for the required phenyl migration from nitrogen (owing to the multiple bond character inherent in such N–Ph linkages).<sup>13</sup> A more likely mechanism consistent with these data involves initial O-coordination of N<sub>2</sub>O to the coordinatively unsaturated Hf center followed by rate-determining hydride (or aryl) migration with concomitant loss of N<sub>2</sub> (Scheme 1).<sup>14</sup> The apparent differing modes of interaction for these isoelectronic molecules (N<sub>2</sub>O vs. RN<sub>3</sub>, R<sub>2</sub>CN<sub>2</sub>) with Group 4 metallocene derivatives may well be attributable to steric factors.

Since oxygen-transfer reactions using Group 4, d<sup>0</sup> metals with the common oxidants O<sub>2</sub><sup>15</sup> and *t*-BuOOH (TBHP)<sup>16,17</sup> comprise an important, well-studied class,<sup>18</sup> it is worth noting an interesting feature of these reactions (that contrasts with ours using N<sub>2</sub>O): they proceed via intermediate *alkylperoxy ligands and, often, derived radicals*.<sup>15,16</sup> Furthermore, the thermal generation of radicals in these systems can limit their synthetic utility: TBHP converts many Cp\*<sub>2</sub>HfR<sub>2</sub> complexes to the corresponding Cp\*<sub>2</sub>Hf(OR)(O-*t*-Bu) but is ineffectual in oxidizing the aryl ligand of **3** due to O–O homolysis of the isolable Cp\*<sub>2</sub>Hf(OO-*t*-Bu)(Ph) intermediate to give **4** (compare this with eq 5).<sup>16a</sup>

In summary, these findings are significant because they demonstrate a fundamentally new mode of nitrous oxide reactivity with transition-metal complexes: *direct O-atom transfer from N<sub>2</sub>O to metal–ligand bonds* instead of the commonly observed O-abstraction to form metal–oxo species.<sup>4</sup> We are currently

(11) **4**, **5**, and **6** can be prepared independently: **3** + H<sub>2</sub>O → **4**; **1** + HOPH → **5**; **5** + H<sub>2</sub>O → **6**. See ref 9 for details.

(12) Thermal decomposition with loss of benzene occurs on heating **4** to 140 °C.

(13) (a) Pauling, L. *The Nature of the Chemical Bond*, 3rd ed.; Cornell University: Ithaca, NY, 1960; pp 280, 296. (b) Streitwieser, A., Jr.; Heathcock, C. H. *Introduction to Organic Chemistry*, 3rd ed.; Macmillan: New York, 1985; p 691ff.

(14) As pointed out by a referee, there is no precedent for O-coordinated N<sub>2</sub>O, but it is reasonable that highly oxophilic early-metal d<sup>0</sup> centers would promote this binding mode.<sup>14a,b</sup> Nevertheless, initial N-coordination and rearrangement or concerted rearrangement/insertion should be considered as a mechanistic possibility. Attempts to measure an isotope effect using Cp\*<sub>2</sub>Hf(D)(Ph) resulted in scrambling of the deuterium into the aryl positions before O-insertion occurred, suggesting a possible benzyne intermediate in the reaction shown in eq 5.<sup>14c</sup> (a) Tuan, D. F.-T.; Hoffmann, R. *Inorg. Chem.* **1985**, *24*, 871. (b) Bottomley, F.; Brooks, W. V. F. *Ibid.* **1977**, *16*, 501. (c) Vaughan, G. A.; Hillhouse, G. L.; Buchwald, S. L., manuscript in preparation.

(15) (a) Lubben, T. V.; Wolczanski, P. T. *J. Am. Chem. Soc.* **1985**, *107*, 701. (b) Lubben, T. V.; Wolczanski, P. T. *Ibid.* **1987**, *109*, 424. (c) Brindley, P. B.; Scotton, M. J. *J. Chem. Soc., Perkin Trans. 2* **1981**, 419. (d) Blackburn, T. F.; Labinger, J. A.; Schwartz, J. *Tetrahedron Lett.* **1975**, 3041.

(16) (a) van Asselt, A.; Santarsiero, B. D.; Bercaw, J. E. *J. Am. Chem. Soc.* **1986**, *108*, 8291. (b) Sharpless, K. B.; Woodard, S. S.; Finn, M. G. *Pure Appl. Chem.* **1983**, *55*, 1823. (c) Also, ref 18.

(17) Shell process for propylene epoxidation: (a) Sheldon, R. A. In *Aspects of Homogeneous Catalysis*; Ugo, R., Ed.; Reidel: Dordrecht, 1981; Vol. 4, p 3. (b) Shell Oil Br. Patent 1 249 079, 1971. Shell Oil U.S. Patent 3 923 843, 1975.

(18) Applications in organic synthesis: (a) Finn, M. G.; Sharpless, K. B. In *Asymmetric Synthesis*; Morrison, J. D., Ed.; Academic: New York, 1985; Vol. 5, p 247. (b) Sharpless, K. B.; Behrens, C. H.; Katsuki, T.; Lee, A. W. M.; Martin, V. S.; Takatani, M.; Viti, S. M.; Walker, F. J.; Woodard, S. S. *Pure Appl. Chem.* **1983**, *55*, 589. (c) Sharpless, K. B.; Verhoeven, T. R. *Aldrichim. Acta* **1979**, *12*, 63.

exploring the scope of the reactivity of nitrous oxide with other d<sup>0</sup> organometallic complexes, and these studies will be the topic of future reports.

**Acknowledgment.** Financial support from the National Science Foundation (Grant CHE-8520329) and the donors of the Petroleum Research Fund, administered by the American Chemical Society (17718-AC3), is appreciated. The NMR facilities were supported in part through the University of Chicago Cancer Center Grant (NIH-CA-14599).

**Supplementary Material Available:** Tables of analytical, NMR, and IR data; synthetic and experimental details; and kinetic data (4 pages). Ordering information is given on any current masthead page.

## The First Structural Characterization of a Dimeric Lithium Ketone Enolate–Lithium Diisopropylamide Complex

Paul G. Williard\* and Mark J. Hintze

Department of Chemistry, Brown University  
Providence, Rhode Island 02912

Received February 27, 1987

While attempting to obtain information concerning the effects of chelation on the aggregation state of lithium ketone enolates, we discovered a new dimeric, lithium enolate–lithium amide base complex. We obtained the structure of this dimeric complex by X-ray diffraction analysis. This dimeric complex may occur commonly in solution; hence, the general structure of the dimer is likely to have mechanistic implications in the reaction of ketones with lithium amide bases.

When a heptane solution of the ketone **1** is added to a suspension of freshly prepared lithium diisopropylamide (LDA) in the same solvent, a homogenous solution is formed after only 0.5 equiv of the ketone has been added. If the addition of ketone to the base is stopped after the homogenous solution is obtained and if the reaction mixture is subsequently placed in a freezer maintained at –20 °C, large transparent crystals are obtained. In an alternative procedure, we added a full stoichiometric amount of ketone to the amide base, followed by addition of a second full equivalent of *n*-BuLi. This procedure also yields crystals of the same composition. We carried out low-temperature (~–100 °C) diffraction analysis of these crystals according to our standard protocol.<sup>1</sup> The structure of a dimeric, enolate–LDA complex was obtained.<sup>2</sup> This is depicted in Figure 1 as the aggregate **2**.

Two computer generated plots of the dimer are shown in Figure 1 in order to emphasize its stereochemistry. The perspective of the molecule differs by 90° rotation about a horizontal axis in the two plots. In the top plot, the seven-membered chelate rings, made up of an enolate oxygen, a lithium atom, and the silyl ether oxygen, are clearly discernible. In the bottom plot, the slight curvature of the fused, four-membered ring skeleton of the dimer is apparent. It is noteworthy that the silyl ether oxygens coordinate with lithium atoms despite the steric bulk of the *tert*-butyldimethylsilyl group. This coordination is contrary to recent observations that silyl ethers are poor electron donors.<sup>3</sup>

(1) Williard, P. G.; Carpenter, G. B. *J. Am. Chem. Soc.* **1986**, *108*, 462.

(2) The enolate–LDA complex underwent spontaneous resolution and crystallized in the noncentrosymmetric, monoclinic space group *P*2<sub>1</sub> with unit cell parameters *a* = 12.282 (3) Å, *b* = 10.911 (3) Å, *c* = 17.606 (8) Å, and β = 92.67 (3)°. The unit cell contained two asymmetric units of molecular formula [(C<sub>13</sub>H<sub>27</sub>SiO<sub>2</sub>Li)·(C<sub>6</sub>H<sub>14</sub>NLi)]<sub>2</sub> in a volume of 2356.8 (1.3) Å<sup>3</sup>. This produces a calculated density of 1.01 g·cm<sup>-3</sup>. A total of 4100 reflections were recorded by using the θ:θ scan routine and graphite monochromated Mo Kα radiation in the range 3.5° ≤ 2θ ≤ 45°. The final agreement factors are *R* = 0.0414 and *R*<sub>w</sub> = 0.0493 for 450 parameters and 3557 unique, observed reflections. A complete description of the crystallographic parameters is submitted as Supplementary Material.

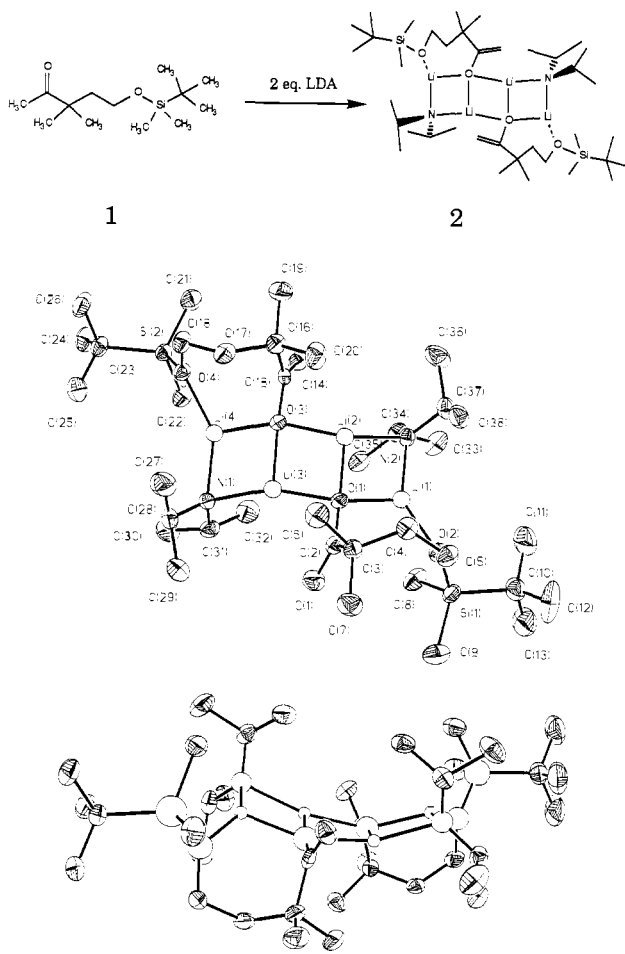


Figure 1.

Recent experimental evidence has accumulated to suggest the existence of aggregates of enolates and amide bases in solution.<sup>4</sup> This evidence is in addition to the considerable existing evidence for aggregation of enolates with secondary amines both in solution and in the solid state.<sup>5</sup> Since the synthetic procedure for the formation of lithium enolates is routinely carried out by addition of the carbonyl component to excess amide base, the opportunity to form dimeric complexes such as **2** persists throughout the first half of the reaction in which the enolate is being produced. We have observed solubility behavior identical with that described above for several different ketones. Therefore, we suggest that the formation of dimeric aggregates similar to **2** generally occurs when the stoichiometry is correct. Structure **2** can serve as a useful model for the enantioselective reactions which utilize chiral lithium amide bases.<sup>6</sup>

Crystal structures of ketone enolate aggregates have been reported for several synthetically useful metal cations including Li, Na, K, and Mg.<sup>7</sup> These structures, along with the structure of

(3) (a) Kahn, S. D.; Keck, G. E.; Hehre, W. J. *Tetrahedron Lett.* **1987**, 279. (b) Keck, G. E.; Castellino, S. *Tetrahedron Lett.* **1987**, 281.

(4) (a) Strazewski, P.; Tamm, Ch. *Helv. Chim. Acta* **1986**, 69, 1041. (b) Tamm, Ch.; Gamboni, R. *Helv. Chim. Acta* **1986**, 69, 615. (c) Miller, D. J.; Saunders, W. H. Jr *J. Org. Chem.* **1982**, 47, 5039. (d) Helmchen, G.; Grottemeier, G.; Schmierer, R.; Selim, A. *Angew. Chem.*, **1981**, 93, 209.

(5) Laube, T.; Dunitz, J. D.; Seebach, D. *Helv. Chim. Acta* **1985**, 68, 1373 and references therein.

(6) (a) Whitesell, J. K.; Felman, S. W. *J. Org. Chem.* **1980**, 45, 755. (b) Shirai, R.; Tanaka, M.; Koga, K. *J. Am. Chem. Soc.* **1986**, 108, 543. (c) Simkins, N. *J. Chem. Soc., Chem. Commun.* **1986**, 88. (d) Eleveld, M. B.; Hogeveen, H. *Tetrahedron Lett.* **1986**, 631.

(7) (a) Amstutz, R.; Schweizer, W. B.; Seebach, D.; Dunitz, J. D. *Helv. Chim. Acta* **1981**, 64, 2617. (b) Williard, P. G.; Carpenter, G. B. *J. Am. Chem. Soc.* **1985**, 107, 3345. (c) Jastrzebski, J. T. B. H.; van Koten, G.; Christophersen, M. J. N.; Stam, C. H. *J. Organomet. Chem.* **1985**, 292, 319. (d) Williard, P. G.; Salvino, J. M. *J. Chem. Soc., Chem. Commun.* **1986**, 153. (e) See ref 1.

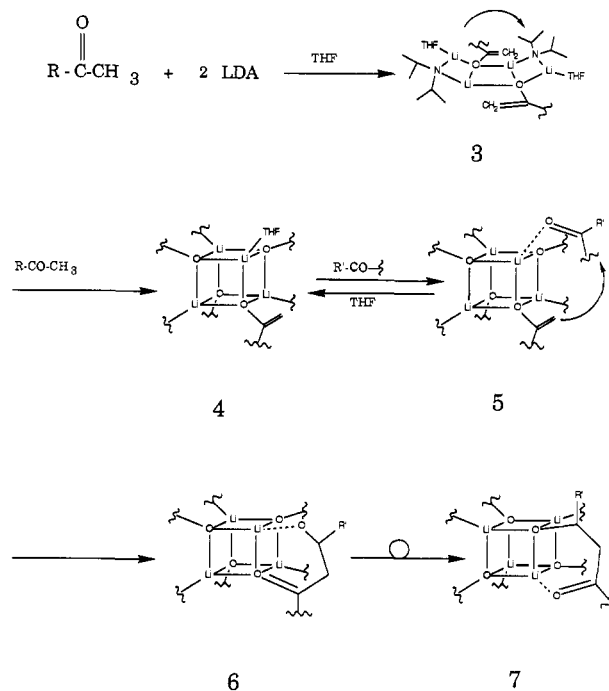


Figure 2.

the Li aldolate aggregate which we reported,<sup>8</sup> support the generalized depiction of the aldol reaction<sup>9</sup> given in Figure 2. Crystal structures corresponding to the intermediates **3**, **4**, **5**, and **7** currently exist. Investigators have also increasingly resorted to the use of aggregates to explain C- vs. O-alkylation ratios or the stereochemistry of enolate reaction products. Recent examples include the alkylation of lithioisobutyrophenone<sup>10a,b</sup> or lithium dimethylhydrazone enolates<sup>10c,d</sup> and the aldol reaction product of lithium norbornenone enolate with the parent ketone.<sup>10e</sup> Despite this growing use of enolate aggregates to explain observed chemistry, little is known about the mechanism by which enolate aggregates themselves are formed or about their structures.

Tetrameric enolate aggregates such as **4** have previously been shown to exist in solution.<sup>11</sup> The significance of the dimeric aggregate reported herein is that it represents a logical precursor to the tetramer **4**. We note that the slight bow shape of the dimeric enolate/amide aggregate is already along the pathway for closing to the tetramer **4**. Thus, the dimer characterized herein and generalized as structure **3** in Figure 2 represents an extension as well as an integral part of this synthetically important reaction sequence.

Undoubtedly the chelation in **2** serves to stabilize the dimeric aggregation state of this species. However, it is noteworthy that a nonchelated, ladder-type structure analogous to **3**, in which a THF oxygen coordinates to the terminal lithium atom, has been reported for lithium di-*tert*-butyl phosphide-THF complex.<sup>12</sup> Thus we feel justified in proposing the occurrence of this type of aggregate in the general reaction scheme in Figure 2 where chelation

(8) Williard, P. G.; Salvino, J. M. *Tetrahedron Lett.* **1985**, 3931.

(9) Seebach, D.; Amstutz, R.; Dunitz, J. D. *Helv. Chim. Acta* **1981**, 64, 2621.

(10) (a) Jackman, L. M.; Dunne, T. S. *J. Am. Chem. Soc.* **1985**, 107, 2805. (b) Jackman, L. M.; Lange, B. C. *J. Am. Chem. Soc.* **1981**, 103, 4494. (c) Collum, D. B.; Wanat, R. A. *J. Am. Chem. Soc.* **1985**, 107, 2078. (d) Collum, D. B.; Kahne, D.; Gut, S. A.; DePue, R. T.; Mohamadi, F.; Wanat, R. A.; Clardy, J.; Van Duynne, G. *J. Am. Chem. Soc.* **1984**, 106, 4865. (e) Horner, J. H.; Vera, M.; Grutzner, J. B. *J. Org. Chem.* **1986**, 51, 4212.

(11) (a) Jackman, L. M.; Lange, B. C. *Tetrahedron* **1977**, 33, 2737. (b) Jackman, L. M.; Szeverenyi, N. M. *J. Am. Chem. Soc.* **1977**, 99, 4954. (c) Jackman, L. M.; Haddon, R. C. *J. Am. Chem. Soc.* **1973**, 95, 3687.

(12) (a) Jones, R. A.; Stuart, A. L.; Wright, T. C. *J. Am. Chem. Soc.* **1983**, 105, 7459. (b) Another "ladder"-type structure is reported for lithium pyrrolidide solvated by pentamethyldiethylenetriamine, see: Armstrong, D. R.; Barr, D.; Clegg, W.; Mulvey, R. E.; Reed, D.; Snaith, R.; Wade, K. *J. Chem. Soc., Chem. Commun.* **1986**, 869.

is not possible and a donating solvent, such as THF, must be invoked.

At present, X-ray diffraction analysis provides the most efficient method for obtaining structural models for the reactions in Figure 2. Consequently, we will continue to seek structural information for additional molecular aggregates that will elaborate on the complexes depicted in Figure 2 and expand upon the role of "molecular preorganization"<sup>13</sup> and/or "complex induced proximity effects"<sup>14</sup> in the aldol reaction.

**Acknowledgment.** We thank Dr. Terry Rathman, Lithco Corp., for providing us with a generous supply of *tert*-butyldimethylsilyl chloride. The X-ray equipment was purchased with an instrument grant from the NSF (CHE-8206423). This work was supported by the National Institutes of Health through Grant GM-35982.

**Supplementary Material Available:** Full crystallographic details including atomic coordinates, thermal parameters, bond angles, bond lengths, and a thermal ellipsoid plot (8 pages). Ordering information is given on any current masthead page.

(13) Cram, D. J. *Angew. Chem., Int. Ed. Engl.* 1986, 25, 1039.

(14) Beak, P.; Meyers, A. I. *Acc. Chem. Res.* 1986, 19, 356.

## Parahydrogen and Synthesis Allow Dramatically Enhanced Nuclear Alignment

C. Russell Bowers and D. P. Weitekamp\*

Contribution No. 7578, Arthur Amos Noyes Laboratory of Chemical Physics, California Institute of Technology Pasadena, California 91125

Received April 23, 1987

Recently we have predicted that very large nuclear spin magnetizations can be obtained on molecules formed by molecular addition of parahydrogen ( $p\text{-H}_2$ ) such that the dihydrogen protons become magnetically inequivalent.<sup>1</sup> In this communication we report the experimental observation of this effect. The reaction studied is the hydrogenation of acrylonitrile,  $\text{CH}_2\text{CHCN}$ , to propionitrile,  $\text{CH}_3\text{CH}_2\text{CN}$ , catalyzed by tris(triphenylphosphine)rhodium(I) chloride (Wilkinson's catalyst<sup>2</sup>) at ambient temperature and pressure. Large transient proton nuclear magnetic resonance (NMR) signals are observed both in propionitrile transitions and in the hydride region<sup>2,3</sup> of the hydrogenated catalyst.

Figure 1a shows the proton NMR spectrum ( $\nu_0 = 200$  MHz) of a deuteriobenzene solution 0.76 M in acrylonitrile and 0.035 M in  $\text{Rh}(\text{PPh}_3)_3\text{Cl}$  obtained by Fourier transformation of the free-induction decay after a  $6 \mu\text{s}$   $\pi/2$  pulse. Figure 1b was obtained from the same sample after  $\text{H}_2$  enriched to 50% in the para nuclear spin state was bubbled for 1.1 s through a capillary submerged in the spinning NMR sample, ending 0.8 s before the rf pulse to allow the turbulence to subside. Figure 1c was obtained 200 s later with no further addition of  $\text{H}_2$  and shows that the reaction-induced state which leads to the intense antiphase multiplets of Figure 1b is transient in nature. When the time between the  $\text{H}_2$  burst and the rf pulse is varied, an exponential decay of the antiphase amplitude is observed with a time constant  $T_{1J}^* = 7 \pm 2$  s, where the subscript  $J$  indicates the nature of the nonequilibrium population differences present<sup>1</sup> and distinguishes this quantity from the usual relaxation time  $T_1$  for longitudinal magnetization. The superscript indicates the chemical species. The frequencies of the transient lines are those expected for the hydrogenation product propionitrile. Since the propionitrile is

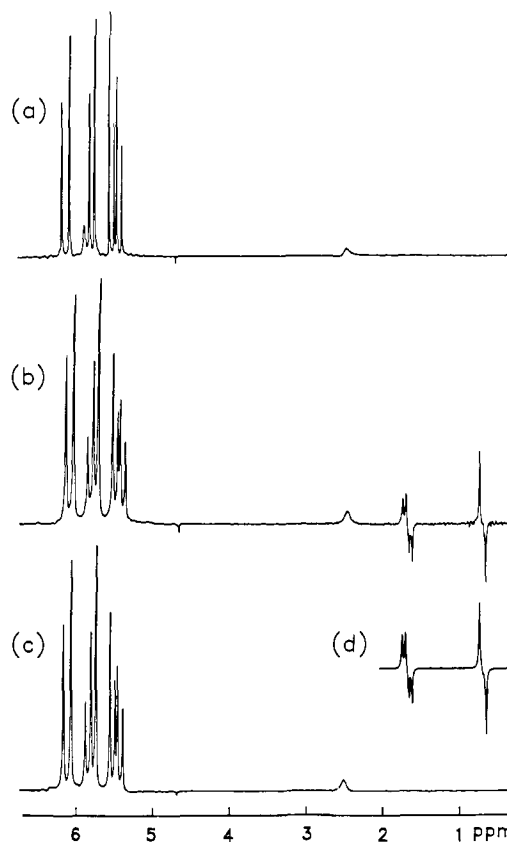


**Figure 1.** Demonstration that parahydrogen and synthesis allow dramatically enhanced nuclear alignment. Part (a) shows the proton NMR spectrum prior to the reaction. The intense lines are due to the acrylonitrile substrate. Part (b) was obtained subsequent to the hydrogenation to propionitrile but prior to spin-lattice equilibration. The large antiphase propionitrile multiplets in response to a  $\pi/4$  pulse are observed only with para-enriched  $\text{H}_2$  as reagent. Part (c) is the spectrum of the equilibrated sample and shows that the signal of (b) was a large transient enhancement. Part (d) is a line shape simulation demonstrating the agreement of the theory of ref 1 with the experiment of part (b). The line width is 3.5 Hz due to inhomogeneity of the field, which is degraded by the  $\text{H}_2$  capillary.

a stable product, the transient nature of the enhanced NMR response must be a spin-lattice relaxation process from a highly ordered state, which upon irradiation gives signals orders of magnitude greater than the signal due to the equilibrium magnetization of the propionitrile (compare parts b and c of Figure 1).

The expected spectrum may be deduced from the previous theory<sup>1</sup> with minor extensions necessitated by the present system. The  $\text{H}_2$  nuclear spin density operator is  $\gamma = (1/4) - fI_1 \cdot I_2$ , where  $f = (1/3)(4x_p - 1)$  and  $x_p$  is the fraction of  $\text{H}_2$  which is  $p\text{-H}_2$ . The  $\text{H}_2$  gas was passed over a nickel-silica catalyst<sup>4</sup> held in a liquid  $\text{N}_2$  bath, in order to achieve  $f = 0.34$ , and then warmed to room temperature before use, presumably without significant interconversion of ortho and para states. The multiplet intensities can be predicted analytically in the weak coupling limit. Instead of the usual paramagnetic (3/4,3/2,3/4) pattern for the methyl group (normalized to sum to 3 at zero K), one finds (1/8,0,-1/8) for the  $f = 1$  limit. Similarly, for the methylene group the usual (1/4,3/4,3/4,1/4) multiplet becomes (1/16,1/16,-1/16,-1/16) with interference cancelling two of the three contributions to the inner lines. For comparison to the experiment of Figure 1b an exact numerical simulation of the propionitrile line shape was made (Figure 1d). The initial condition was obtained by deleting<sup>1</sup> oscillating zero quantum density matrix elements, which appear when the  $\text{H}_2$  initial condition is expressed in the five-spin eigenbasis of the product. The weak coupling argument given above is

(1) Bowers, C. R.; Weitekamp, D. P. *Phys. Rev. Lett.* 1986, 57, 2645-48.

(2) Osborn, J. A.; Jardine, F. H.; Young, J. F.; Wilkinson, G. J. *J. Chem. Soc. A* 1966, 1711-1732.

(3) Meakin, P.; Jesson, J. P.; Tolman, C. A. *J. Am. Chem. Soc.* 1972, 95, 3240-3242.

(4) Silvera, I. F. *Rev. Mod. Phys.* 1968, 52, 393-452.